DOI:10.33266/1024-6177-2026-71-6-156-164

R. Bouchouareb[1], K. Hadj Amor[1], S. Berhab[2]

Parametric Study of an Antenna Detecting Breast Cancer

[1] Department of Networks and Telecommunications, Oum El Bouaghi University, Institute of Technology, Oum El Bouaghi, Algeria

[2] Higher National School of Telecommunication and Information and Communication Technologies, Si Radouane City, Oran, Algeria

Contact person : Rachida Bouchouareb, e-mail: bouchouareb.rachida@univ-oeb.dz

ABSTRACT

Relevance: Cancer diagnosis typically involves a comprehensive medical evaluation, including a physical examination, laboratory tests, and imaging techniques such as X-rays, ultrasound, CT scans, magnetic resonance imaging (MRI), and mammography. Biopsies are also performed to examine suspicious tissue samples. However, these traditional diagnostic methods have several limitations.
Purpose: Conventional breast imaging techniques suffer from limitations related to radiation exposure, discomfort, limited sensitivity in dense tissue, or high cost. This study investigates a non-ionizing, antenna-based microwave detection system as a preliminary mass-screening tool, focusing on its ability to identify dielectric inhomogeneities associated with malignant breast tumors and to differentiate normal from potentially pathological tissue.
Material and methods: Among new methods, patch antennas are a promising solution. In this study, we propose a patch antenna system for breast cancer detection. The parameters investigated using High-Frequency Structure Simulator (HFSS) software include the distance between the antenna and the breast, tumor size, tumor location, and tumor number.
Results: Simulation results of the proposed antenna for several cases are presented and analyzed. The results show that optimal reflectivity (S11) and voltage standing wave ratio (VSWR) characteristics are achieved with a distance of 10 cm between the transmitting (TX) and receiving (RX) antennas. Regarding tumor location, the highest S11 value is achieved when the tumor is located in the center of the breast. For tumor thickness, six cases were studied, revealing that larger tumors yield higher S11 values. Furthermore, the number of tumors also affects the S11 parameter, increasing as the tumor number decreases.
Conclusion: This study demonstrates the influence of tumor presence, position, size, and number on key antenna parameters (S11, S21, and VSWR), highlighting the potential of microwave antenna systems for breast cancer detection.

Keywords: *patch antenna, medical antenna, breast cancer, HFSS, S11, VSWR*

For citation: R. Bouchouareb, K. Hadj Amor, S. Berhab. Parametric Study of an Antenna Detecting Breast Cancer. Medical Radiology and Radiation Safety. 2026;71(6):156–164. DOI:10.33266/1024-6177-2026-71-6-156-164

DOI:10.33266/1024-6177-2026-71-6-156-164

R. Bouchouareb[1], K. Hadj Amor[1], S. Berhab[2]

ПАРАМЕТРИЧЕСКАЯ ДИАГНОСТИКА РАКА МОЛОЧНОЙ ЖЕЛЕЗЫ С ИСПОЛЬЗОВАНИЕМ ПАТЧ-АНТЕНН

[1] Department of Networks and Telecommunications, Oum El Bouaghi University, Institute of Technology, Oum El Bouaghi, Algeria

[2] Higher National School of Telecommunication and Information and Communication Technologies, Si Radouane City, Oran, Algeria

Контактное лицо: Rachida Bouchouareb, e-mail: bouchouareb.rachida@univ-oeb.dz

АННОТАЦИЯ

Актуальность: Диагностика рака обычно включает в себя комплексное медицинское обследование, в том числе физический осмотр, лабораторные анализы и методы визуализации, такие как рентгенография, ультразвуковое исследование, компьютерная томография (КТ), магнитно-резонансная томография (МРТ) и маммография. Также проводятся биопсии для исследования подозрительных образцов тканей. Однако эти традиционные методы диагностики имеют ряд ограничений.
Цель: Традиционные методы визуализации молочной железы страдают от ограничений, связанных с радиационным облучением, дискомфортом, ограниченной чувствительностью в плотных тканях или высокой стоимостью. В этом исследовании изучается неионизирующая система обнаружения микроволнового излучения на основе антенны в качестве предварительного инструмента массового скрининга, с акцентом на ее способность выявлять диэлектрические неоднородности, связанные со злокачественными опухолями молочной железы, и дифференцировать нормальную ткань от потенциально патологической.
Материал и методы: Среди новых методов перспективным решением являются патч-антенны. В этом исследовании мы предлагаем систему патч-антенн для обнаружения рака молочной железы. Параметры, исследованные с помощью программного обеспечения High-Frequency Structure Simulator (HFSS), включают расстояние между антенной и молочной железой, размер опухоли, локализацию опухоли и количество опухолей.
Результаты: Представлены и проанализированы результаты моделирования предлагаемой антенны для нескольких случаев. Результаты показывают, что оптимальные характеристики отражательной способности (S11) и коэффициента стоячей волны по напряжению (VSWR) достигаются при расстоянии 10 см между передающей (TX) и приемной (RX) антеннами. Что касается расположения опухоли, то наибольшее значение S11 достигается, когда опухоль расположена в центре молочной железы. Для исследования толщины опухоли было изучено шесть случаев. Показано, что более крупные опухоли дают более высокие значения S11. Кроме того, количество опухолей также влияет на параметр S11, увеличиваясь по мере уменьшения количества опухолевых узлов.

Заключение: Данное исследование демонстрирует влияние наличия, положения, размера и количества опухолей на ключевые параметры антенны (S11, S21 и VSWR), подчеркивая потенциал микроволновых антенных систем для обнаружения рака молочной железы.

Ключевые слова: *патч-антенна, медицинская антенна, рак молочной железы, HFSS, S11, КСВ*

Для цитирования: R. Bouchouareb, K. Hadj Amor, S. Berhab. Параметрическая диагностика рака молочной железы с использованием патч-антенн // Медицинская радиология и радиационная безопасность. 2026. Т. 71. № 6. С. 156–164. DOI:10.33266/1024-6177-2026-71-6-156-164

1. Introduction

Medical imaging involves the visualization of human tissues and organs to monitor both normal and abnormal anatomy and physiology [1–2]. Non-ionizing microwave techniques avoid radiation risks associated with mammography, offer painless scanning without breast compression, and support frequent use for early detection. They exploit dielectric contrasts between healthy and cancerous tissues for preliminary triage, reducing unnecessary follow-up exams [3–5].

This approach targets mass screening to flag suspicious cases for confirmatory tests like ultrasound or MRI, rather than standalone diagnosis. Systems like SAFE demonstrate potential in identifying malignancies early while triaging true negatives [4–6].

Medical patch antennas are specialized electronic devices designed to detect tissue abnormalities associated with cancer by exploiting the electromagnetic properties of biological tissues [7–9]. These antennas are placed on or near the human body, where they interact with surrounding tissues. The patch antenna detects variations in local electromagnetic properties caused by the presence of tumors or cellular changes [10–11]. Consequently, the radiation characteristics of antennas in microwave systems may serve as a complementary or alternative technique to conventional clinical methods for cancer diagnosis[12–13].

Breast cancer is a significant health issue among women and ranks as the second leading cause of cancer-related deaths [14–15]. It arises from malignant transformations in the cells of the breast, either in the ducts (carrying milk from glands to the nipple) or in the lobules [16–18]. These cancers can remain localized (*in situ*) or infiltrate surrounding tissues and organs [19–20]. Understanding tumor behavior is crucial for early detection and effective treatment.

1.1 Electromagnetic properties of human tissues

Extensive characterization of the dielectric properties of human tissues has long been a focus of research. Early studies by Geddes and Becker (1967) measured the specific resistance of tissues [21], followed by Stuchly et al (1980), who compiled dielectric data across a broad frequency range (10 kHz–10 GHz) [22]. Subsequent contributions by Duck, Larges, and others in the 1990s expanded these datasets, emphasizing *in vivo* measurements over *in vitro* animal-based studies [23]. Where *in vitro* measurements were used, data were often recorded at near-physiological temperatures shortly after tissue excision [24]. Many historical datasets were presented graphically rather than numerically, complicating further analysis. Available tabular data often cover wide frequency ranges and have been standardized for body temperature conditions [25–26].

1.2. Electromagnetic parameters of biological tissues:

- Electrical permittivity (ε in F/m):

$$\varepsilon = \varepsilon_0(\varepsilon' - j\varepsilon''), \quad (1)$$

where $\varepsilon_0 = 1.36 \times 10^{-9}$ F/m is the permittivity of free space, ε' is the real part (permittivity), and ε'' is the imaginary part (dielectric losses) [26].

Table 1

Orders of magnitude of electromagnetic parameters for different biological tissues at different frequencies [27]

Электромагнитные характеристики различных биологических тканей на разных частотах. [27]

	GHz	Conductivity, S/m	Permittivity relative	Losses	Wavelength, mm	Penetration depth, mm
Skin, 5 mm	1	0.88	45.71	0.34	43.71	41.29
	2	1.33	43.52	0.27	22.51	26.47
	10	8.95	33.58	0.48	5.04	2.53
	17	16.75	26.26	0.67	3.28	1.71
	30	25.48	19.24	0.88	2.35	0.99
Grease, 5 mm	1	0.05	5.45	0.18	127.96	232.47
	2	0.08	5.33	0.15	64.773	142.99
	10	0.58	4.61	0.23	13.885	19.59
	17	1.06	4.15	0.27	8.5769	10.21
	30	1.64	3.73	0.29	5.6888	6.29
Muscle, 35 mm	1	0.98	54.81	0.32	39.99	40.68
	2	1.45	53.29	0.24	20.38	26.85
	10	10.63	42.76	0.45	4.479	3.34
	17	20.71	34.06	0.64	2.89	1.56
	30	32.62	25.13	0.86	2.06	0.88
Lung, 85 mm	1	0.47	21.83	0.39	63.02	53.27
	2	0.68	20.79	0.30	32.53	5.70
	10	4.21	16.15	0.47	7.27	5.20
	17	7.81	12.78	0.65	0.71	2.54
	30	11.84	9.54	0.83	3.35	1.48
Heart, 55 mm	1	1.28	59.29	0.39	38.24	32.42
	2	1.91	55.82	0.31	19.83	20.98
	10	11.83	42.24	0.50	4.48	3.01
	17	21.91	32.8	0.71	2.92	1.46
	30	33.17	23.73	0.93	2.09	0.85

- Magnetic permeability (μ, H/m): Represents the material's ability to influence the magnetic field and store or dissipate energy in response to magnetic induction. The permeability varies linearly with magnetic excitation H [28].
- Conductivity (σ, S/m): Indicates the ability of ions in a medium to carry current, resulting from ionic migration under an applied electric field [29].
- Dispersion and attenuation: Biological tissues exhibit dispersive and attenuating behavior due to interactions between electromagnetic waves and matter, including polarization and conduction effects [28]. The complex dielectric constant can be expressed as:

$$\varepsilon_c = \varepsilon - j(\sigma/\omega) \quad (2)$$

or

$$\varepsilon_c = \varepsilon' - j\varepsilon'', \quad (3)$$

where ε' represents the permittivity and ε'' the dielectric losses.

For microstrip antennas, the complex effective dielectric constant ε_{eff} can be approximated as:

$$\varepsilon'_{eff} = \frac{((\varepsilon' + 1)/2) + (\varepsilon' - 1)/2)}{\sqrt{1 + 12h/w}} \quad (4)$$

For the imaginary part ε''_{eff}, a similar approach can be used, taking losses into account:

$$\varepsilon''_{eff} = \frac{((\varepsilon'' + 1)/2) + (\varepsilon'' - 1)/2)}{\sqrt{1 + 12h/w}} \quad (5)$$

$$\varepsilon_{eff} = \varepsilon'_{eff} - j\varepsilon''_{eff} \quad (6)$$

These parameters are essential for designing antennas that accurately interact with human tissues in medical imaging applications.

2. Related works

A large and growing body of research has investigated microwave and antenna-based techniques for breast cancer detection due to their non-ionizing nature and capability for early-stage diagnosis. Recent reviews indicate that ultra-wideband (UWB) and near-field antennas dominate in microwave imaging systems because their broad operational frequency range enhances spatial resolution and dielectric contrast sensitivity [30]. In addition, current trends emphasize compact, wearable, and textile antenna designs that improve patient comfort and system conformability [30].

Several antenna configurations–such as Vivaldi, tapered-slot, and modified microstrip patch designs have been developed to achieve wide bandwidth, high gain, and efficient coupling for imaging applications [31, 32]. Experimental studies confirm successful tumor detection using compact UWB planar antennas in both single-antenna and array setups [32]. Accurate dielectric characterization of breast tissues, based on Debye and Cole–Cole dispersion models, is essential to realistic simulations and phantom fabrication [33].

Moreover, parametric investigations have examined the influence of antenna geometry, substrate permittivity, and ground-plane modifications on impedance bandwidth, radiation behavior, and near-field coupling [34]. While most works primarily focus on electromagnetic performance metrics (S11, gain, and radiation pattern), recent developments integrate optimized antennas into full microwave imaging systems, including portable and wearable prototypes, showing promising detection performance in experimental and phantom tests [35].

3. Methodology

3.1 Basic Breast Structure

In this work, the breast is modeled as a half-sphere, and the tumor is modeled as a sphere (see fig. 1). The half-sphere, representing the breast tissue, has a diameter of 70 mm. The model includes three main layers: skin with a thickness of 0.5 mm, fat with a thickness of 0.5 mm, and glandular tissue. The tumor is represented by a sphere with a diameter of 3 mm.

The dielectric properties corresponding to the breast and tumor phantoms at a frequency of 2.45 GHz are presented in table 2 [36–37]. These values are extracted from the Cole–Cole model [38].

3.2 . Basic Antenna Design

3.2.1 Geometric parameters of printed antenna

In order to determine the geometric parameters of a radiating element, it is necessary to calculate:

– The effective permittivity as a function of the patch width *W*.

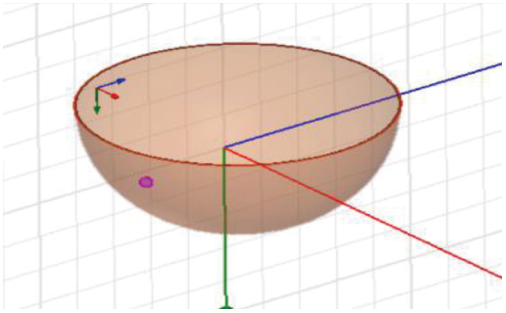


Fig. 1. Hemispherical model of the breast with a tumor

Рис. 1. Полусферическая модель молочной железы с опухолью

Table 2

Units for magnetic properties

Диэлектрические свойства фантомов

	Permittivity ξ, F/m	Conductivity σ, S/m
Skin	38	1.46
Grease	5.6	0.14
Glandular	20	0.3
Tumor	50	4

– The length *L* of the patch as a function of the effective permittivity.

The radiation is based on the actual length as well as the two slits. For the rectangular patch, the length L is extended by two ΔL [39]:

$$\Delta L = 0.412h \left(\frac{\varepsilon_{eff} + 0.3}{\varepsilon_{eff} - 0.3} - 0.3 \right) \left(\frac{w/h + 0.264}{w/h + 0.8} \right) \quad (7)$$

The effective length L_{eff} of the patch is

$$L_{eff} = L + 2\,\Delta L \quad (8)$$

The resonant frequency f_r is [40]:

$$f_r = \frac{c}{2\,L_{eff}\sqrt{\varepsilon_r}} \quad (9)$$

The width of the patch *W* is calculated from the formula (8):

$$f_r = \frac{c}{2f_r} = \sqrt{\frac{\varepsilon_r + 1}{2}} \quad (10)$$

3.2.2 Miniaturization

Antenna miniaturization involves reducing the antenna's dimensions, surface area, and volume while maintaining its performance at the resonant frequency. To ensure optimal functionality, the antenna must be integrated as closely as possible to the associated circuitry.

The detailed parameters of the antenna are presented in the table 3.

Fig. 3 and 4 illustrate the optimized performance of the antenna at the resonant frequency F_{r1} = 2.4 GHz, showing a reflection coefficient of S11 = –44.1687 dB and a Voltage Standing Wave Ratio (VSWR) = 1.0125.

Fig. 5 display the 2D radiation pattern.

4. Simulation & Results

In the following sections, the simulation results of the proposed antenna are presented. The analysis encompasses several study cases that investigate:

- The effect of the distance between the transmitting (TX) and receiving (RX) antennas.

Table 3

Antenna design parameters

Геометрические параметры антенны

Setting	Value, mm	Description
Ls	60	Substrate length
Ws	60	Substrate width
Wp	29.4	Patch length
LP	38	Patch width
Wg	2	Slot width 1
LG	17	Length of slot 1
Wm	1	Slot width 2
Lm	9.5	Length of slot 2
Wa	3	Power line width

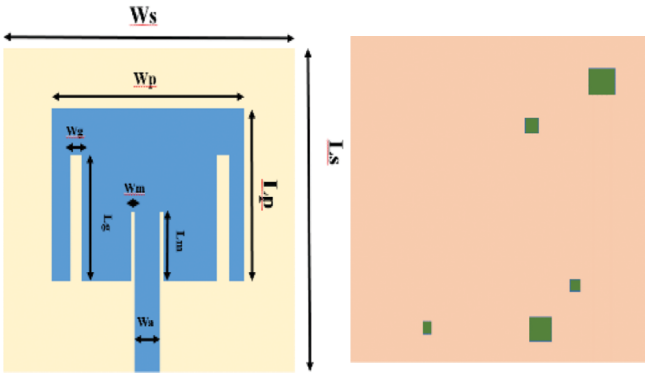


Fig. 2. Illustrates the enhancement of the patch antenna performance through the miniaturization technique, specifically by inserting slots into the antenna structure

Рис. 2. Патч-антенна и заземляющая плоскость

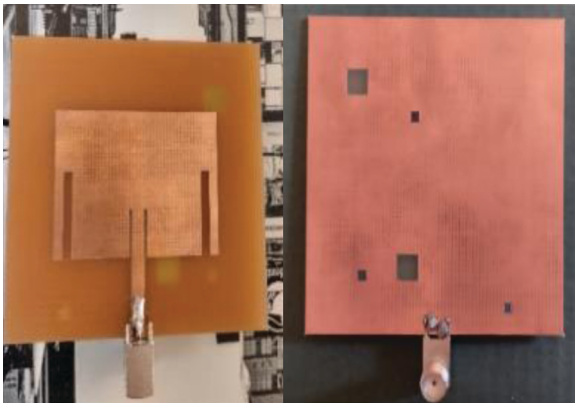


Fig. 3. The manufactured antenna

Рис. 3. Изготовленная антенна

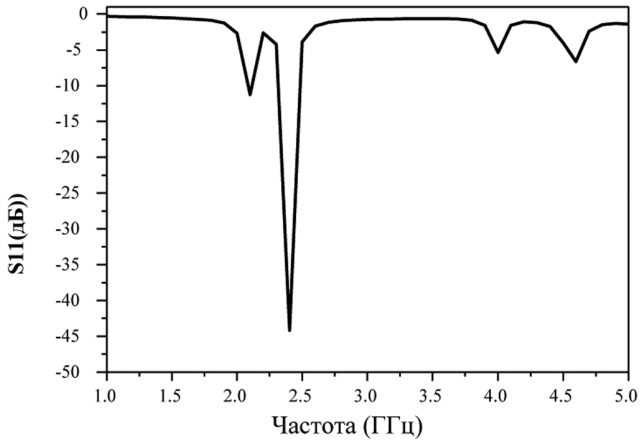
- The tumor location.
- The tumor thickness.
- And the number of tumors.

4.1 The distance

We will study the effect of the location of the antennas (fig. 6, 7, 8).

In this study, six different cases are analyzed by varying the distance between the breast and the RX (receiver antenna) and TX (transmitter antenna). The results, summarized in the table 4, show that the best performance is achieved when the TX antenna is positioned 100 mm from the breast.

The inter-antenna separation affects S21 and slightly modifies S11. VSWR remains near 1, and tumor presence slightly improves impedance matching, indicating that optimal spacing can enhance detection sensitivity.



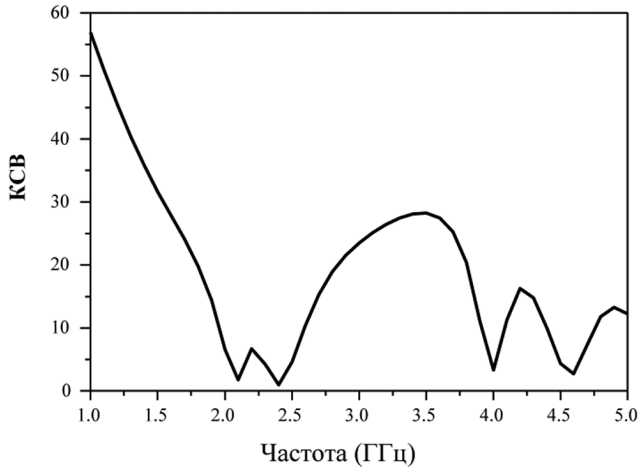


Fig. 4. Reflection coefficient (S11) and VSWR characteristic of the optimized antenna at a frequency of 2.4 GHz

Рис. 4. Коэффициент отражения (S11) и характеристика КСВ оптимизированной антенны на частоте 2,4 ГГц

Table 4

Simulation results for the different distances *f* = 2.4 GHz

Результаты моделирования для различных расстояний *f* = 2.4GHz

Case	With or without tumor	S11, dB	S21, Db	VSWR
TX&RX at 1 cm	With tumor	–14.5236	–37.4961	1.6456
	Without tumor	–14.5597	–37.6532	1.8518
RX at (10 cm)	With tumor	–12.1490	–29.8811	1.7627
	Without tumor	–11.8741	–29.6509	1.8056
TX & RX at 7.5 cm	With tumor	–24.9703	–30.7590	1.1087
	Without tumor	–22.9363	–30.7908	1.1066
TX at (2,630 cm) and RX at 1cm	With tumor	–17.1176	–39.9553	1.2899
	Without tumor	–18.0135	–38.8241	1.2614
TX at (6 cm) and RX at 1 cm	With tumor	–25.7943	–38.2701	1.1226
	Without tumor	–24.2824	–38.1778	1.1454
TX at (10 cm) and RX at 1 cm	With tumor	–40.0409	–41.8836	1.0201
	Without tumor	–32.1090		1.0509

Note: * – S11 Reflection coefficient in dB; ** – S21 Transmission coefficient in dB; *** – VSWR Voltage Standing Wave Ratio; #TX – Transmitter Antenna; ##RX – Receiver Antenna

4.2 The position of the tumor

We analyze the influence of the tumor's position within the breast by considering three cases:

– Tumor positioned on the right side of the breast (see fig. 9).
– Tumor positioned on the left side of the breast (see fig. 10).

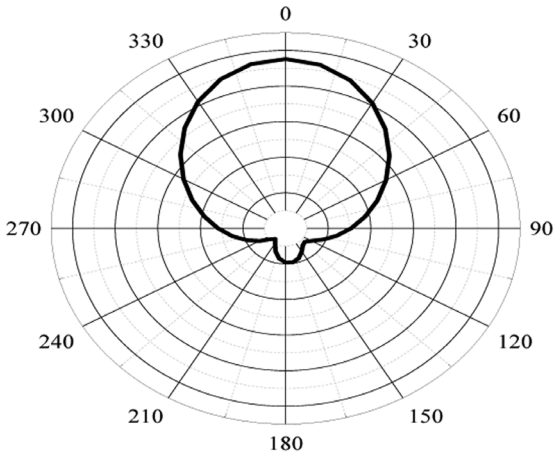


Fig. 5. Display the 2D radiation pattern
Рис. 5. Диаграмма излучения 2D

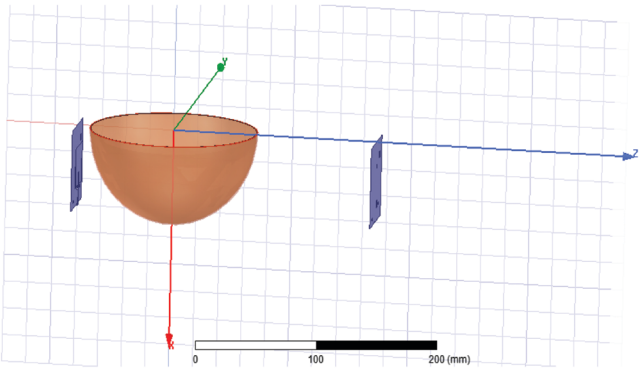


Fig. 6. The receiving antenna on the right is located 10 cm away from the skin of the chest
Рис. 6. Приемная антенна справа расположена на расстоянии 10 см от кожи груди

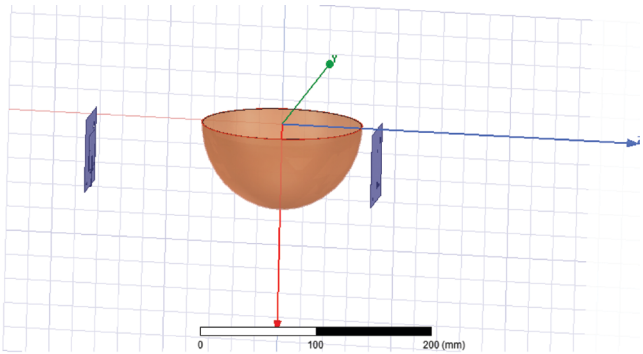


Fig. 7. The transmitting antenna on the left is located 10 cm away from the skin of the chest
Рис. 7. Передающая антенна слева расположена на расстоянии 10 см от кожи груди

– Tumor positioned in the middle of the breast, which has already been studied in the context of varying distances.

The results of S11, S21 and VSWR are summarized in the table 5.

Tumor location strongly influences S11 and S21. Central tumors produce the largest reflection loss, whereas lateral tumors yield stronger transmission attenuation and better antenna matching, suggesting that antenna measurements can assist in tumor localization.

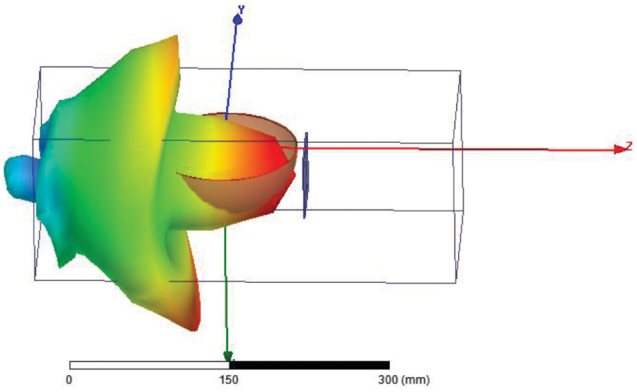


Fig. 8. Three-dimensional antenna radiation pattern (transmitter on the left, receiver on the right)
Рис. 8. Трехмерная диаграмма направленности антенны (передатчик слева, приемник справа)

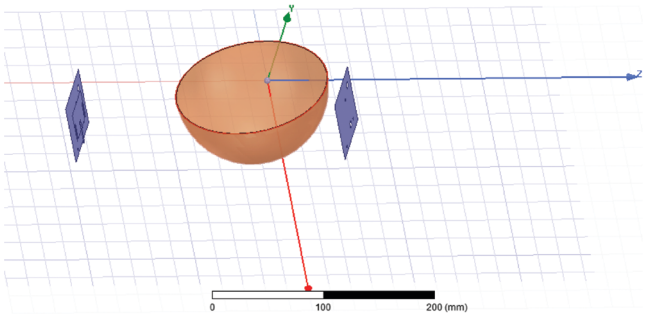


Fig. 9. The tumor is located on the right side of the chest (transmitter on the left, receiver on the right)
Рис. 9. Опухоль расположена на правой стороне груди (передатчик слева, приемник справа)

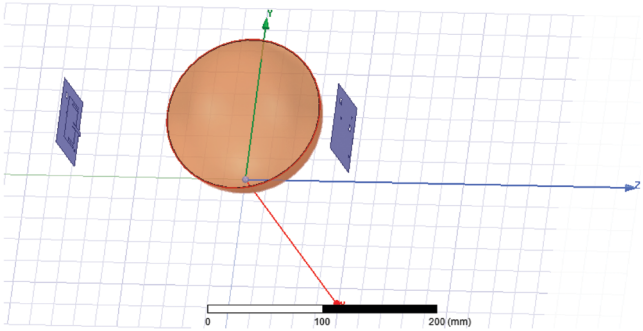


Fig. 10. The tumor is located on the left side of the chest (transmitter on the left, receiver on the right)
Рис. 10. Опухоль расположена на левой стороне груди (передатчик слева, приемник справа)

Table 5

Simulation result for the different tumor positions. *f* = 2.4 GHz

Результаты моделирования для различных положений опухоли *f* = 2.4 GHz

Position	S11, Db	S21, dB	VSWR
Tumor in the middle	–40.0409	–41.8836	1.0201
Tumor on the right	–37.5721	–42.6380	1.0268
Tumor on the left	–34.8402	–43.2957	1.00369

4.3 Tumor thickness

When breast cancer is diagnosed, physicians perform additional tests to determine whether the disease has spread to other parts of the body, a process known as staging. The stage of cancer is a critical factor in determining the appro-

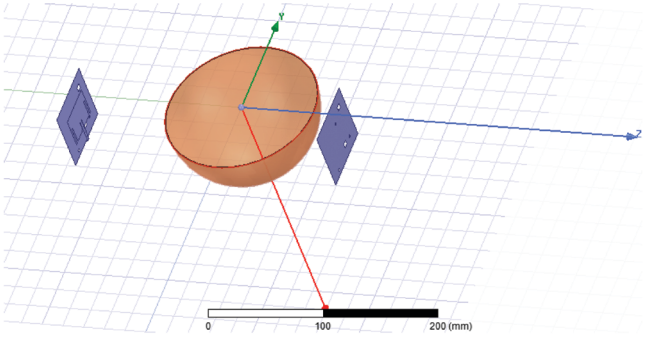


Fig. 11. Tumor with a thickness of 5 mm (transmitter on the left, receiver on the right)

Рис. 11. Опухоль толщиной 5 мм (передатчик слева, приемник справа)

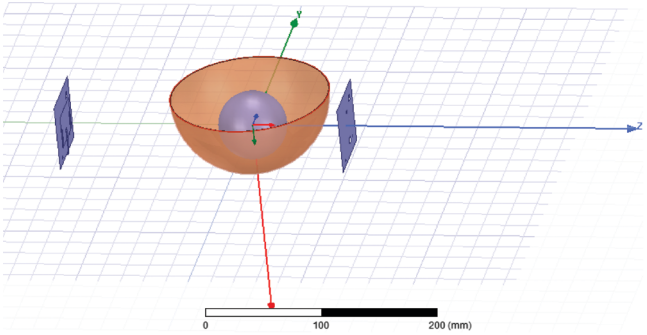


Fig. 12. Tumor with a thickness of 30 mm (transmitter on the left, receiver on the right)

Рис. 12. Опухоль толщиной 30 мм (передатчик слева, приемник справа)

priate treatment plan. Based on the tumor size and the extent of metastasis to nearby organs or lymph nodes, breast cancer is typically classified into four main stages [41].

In this study, the focus is placed on the early detection of breast cancer, specifically targeting stages 1 and 2:

Stage 1: The tumor is no larger than 2 cm in diameter and has not spread beyond the breast.

Stage 2: The tumor measures between 2 and 5 cm and may or may not have spread to the axillary lymph nodes [41].

To simulate realistic scenarios corresponding to these early stages, six representative cases have been analyzed, as illustrated in the fig. 11, 12, 13, 14 and summarized in the accompanying table 6.

Table 6

Simulation result for the different tumor thickness values *f* = 2.4 Ghz

Результаты моделирования для опухолей различной толщины *f* = 2.4 GHz

Thickness, mm	S11, Db	S21, dB	VSWR
5	–32.4592	–41.3440	1.0367
10	–40.4969	–41.5512d	1.0191
15	–35.8497	–42.8578	1.0326
20	–35.1847	–44.4245	1.0354
25	–35.6562	–41.5644	1.0335
30	–42.3030	–40.6747	1.0156

At 2,4 GHz, the reflection coefficient (S11) remains stable between –32 dB and –42 dB for tumor thicknesses of 5–30 mm, while the transmission coefficient (S21) varies between –43 dB and –40 dB, indicating limited energy propagation due to tumor absorption or scattering. S21 shows greater sensitivity to tumor size, particularly in the 2.5–4.5 GHz range, with maximum attenuation reaching –90 dB for diameters of 20–25 mm.

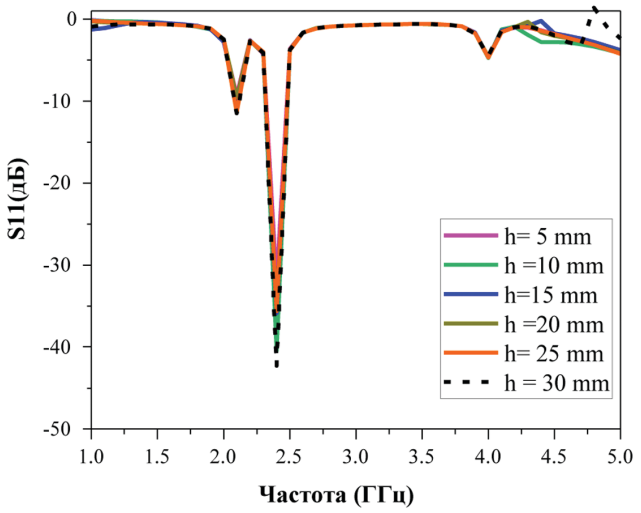


Fig. 13. Reflection coefficient S11 for different tumor thicknesses at *f*=2.4 GHz

Рис. 13. Коэффициент отражения S11 для различной толщины опухоли f=2,4 ГГц

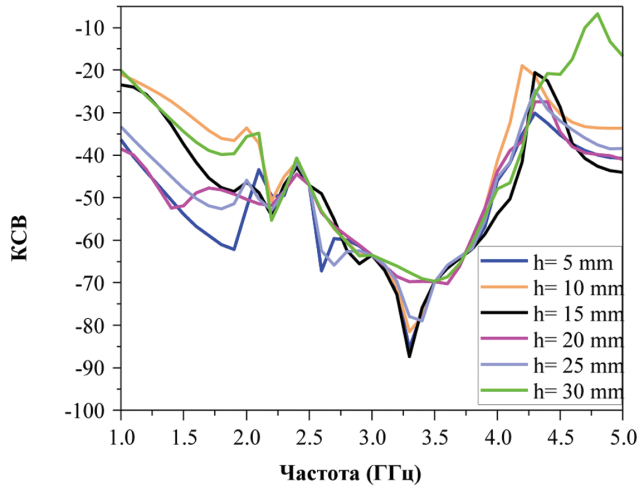


Fig. 14. Transmission coefficient S21 for tumors of various thicknesses at *f* = 2.4 GHz

Рис. 14. Коэффициент пропускания S21 для опухолей различной толщины *f* = 2,4 ГГц

4.4 The number of tumor

In this case, four cases are studied as shown in the fig. 15, 16, 17, 18 and table 7.

Table 7

Simulation result for the different tumor numbers *f* = 2.4 GHz

Результаты моделирования для различного числа опухолей *f*=2,4GHz

	S11, dB	S21, Db	VSWR
Two tumors	–39.6017	–41.4692	1.0212
Three tumors.	–36.7296	–41.5794	1.0296
Four tumors	–42.9260	–41.4146	1.0167
Multiple tumors	–40.5962	–25.9606	1.0188

S11 and S21 decrease with increasing tumor number, especially beyond four tumors, reflecting stronger impedance mismatch and enhanced wave attenuation. VSWR remains near 1, indicating good system matching.

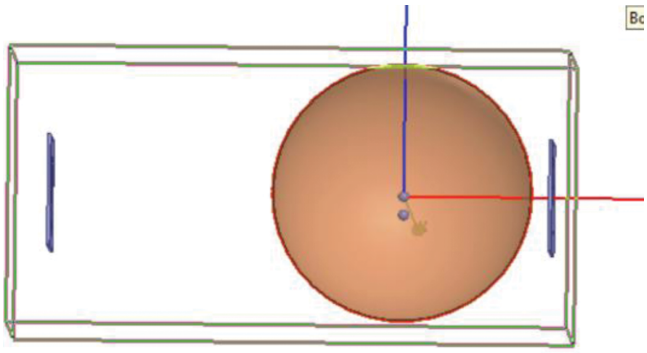


Fig. 15. Case of two tumors in a breast model (transmitter on the left, receiver on the right)

Рис. 15. Случай двух опухолей в модели груди (передатчик слева, приемник справа)

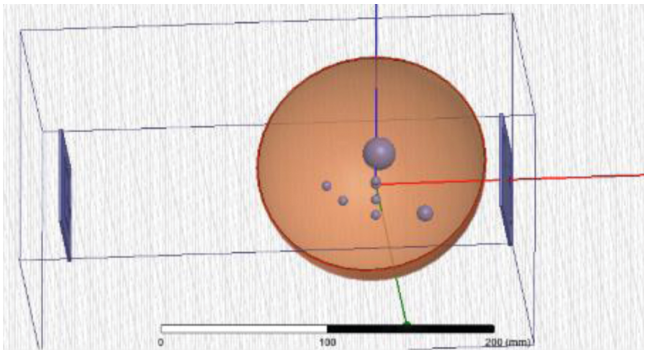


Fig. 16. The case of several tumors in a breast model. (Transmitter on the left, receiver on the right)

Рис. 16. Случай нескольких опухолей в модели груди. (Передатчик слева, приемник справа)

5. Discussion

The study highlights the influence of tumor presence, position, size, and number on antenna parameters (S11, S21, and VSWR):

- **Tumor presence**: it causes stronger reflection (more negative S11) and modifies transmission (S21), while maintaining good impedance matching (VSWR close to 1). These variations can serve as indicators for detection.
- **Tumor position**: localization affects the results. A tumor in the center produces stronger reflection (S11) but weaker transmission attenuation (S21), whereas a tumor on the left results in higher attenuation (S21) and better matching (VSWR). This suggests the possibility of tumor localization through antenna parameter analysis.
- **Tumor thickness and size**:
  Thickness (5–30 mm) has almost no effect on S11, showing its robustness but limiting its use for depth estimation.
  Size strongly influences S21: the larger the diameter, the greater the attenuation, especially between 2.5 and 4.5 GHz. This makes S21 a key parameter for detecting and characterizing tumors.
- **Number of tumors**: at 2.4 GHz, an increase in the number of tumors causes a decrease in both S11 and S21, indicating stronger mismatch and higher attenuation. VSWR remains close to 1, confirming good system adaptation. These results confirm that 2.4 GHz is particularly sensitive to tumor-induced variations, making it a promising frequency for microwave imaging.

In the table 8, we listed comparison between the proposed work and other research.

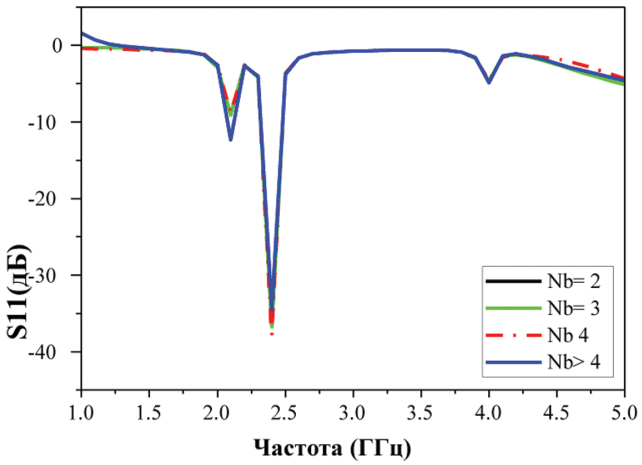


Fig. 17. Reflection coefficient S11 for different numbers of tumors in the breast tissue at f = 2.4 GHz

Рис. 17. Коэффициент отражения S11 для различного количества опухолей в молочной железе при f = 2,4 ГГц

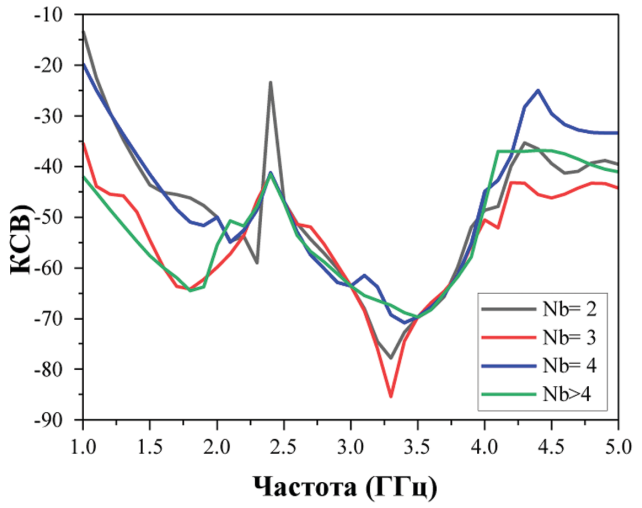


Fig. 18. Transmission coefficient S21 for different numbers of tumors at f = 2.4 GHz

Рис. 18. Коэффициент пропускания S21 для разного количества опухолей при f = 2,4 ГГц

Table 8

Comparison between the proposed work and some important research in the literature

Сравнение данной работы с некоторыми другими примечательными исследованиями

Aspect	Proposed Work	Fawzia et al [42]	Elsheikh et al [43]	Lin et al [44]
Frequency range, GHz	2–2.5	2–11.6	1.8–2.4 and 4–10	1.198–4.055
Substrate/ conductive	FR4 epoxy/ copper	Denim/ fabric	Cotton/roger-fabric	Polyester/ copper
Antenna size, mm^2	38–29.4	31–31	24–41	40–45
Breast phantom	Single layer	Multilayer	Single layer	Multilayer
Max S11 value (–10 dB)	–42.9260	–36	–30	–40
Tumor size, mm	5, 10, 15 and 30	2 and 5	10 and 20	None

Table 8 compares the proposed patch antenna with several notable studies from the literature. The proposed design

operates in the 2–2,5 GHz ISM band, which is both safe and medically approved, unlike other works that use broader and higher frequency ranges. It employs FR4 epoxy with copper, a cost-effective and reliable choice, whereas some studies use textile-based substrates that improve flexibility but may reduce performance. With its compact size (38 × 29.4 mm²), the antenna is well-suited for integration into medical devices, striking a balance between size and performance.

A single-layer breast phantom is used in simulations, offering simplicity compared to multilayer models, though the latter provide higher anatomical accuracy. In terms of performance, the proposed antenna achieves an S11 of –42.9 dB, outperforming other designs that range between –30 dB and –40 dB, thus ensuring excellent impedance matching. Moreover, the design evaluates a wider range of tumor sizes (5–30 mm) than other studies, demonstrating greater adaptability for detecting tumors at different stages.

We clarify that our current phantom model focuses on primary tumor detection and does not account for multifocal disease or nodal involvement, which represents a limitation for staging applications.

However, any suspicious findings identified by the microwave method should be further evaluated using standard medical imaging (mammography, ultrasound, MRI, etc.) and, where appropriate, histological verification of the targeted biopsy under imaging guidance.

Limitations and Future Directions:

- **Homogeneous tumor model.** The current model is simplified and does not capture clinical tumor heterogeneity; future studies will include heterogeneous tumors with calcifications, necrosis, fibrosis, and mixed cell populations.
- **Tumor subtype variability.** Microwave studies show that dielectric contrast persists across major breast cancer subtypes (IDC, ILC, DCIS), though detection sensitivity varies with tumor grade and composition [12, 45, 46].
- **Regional spread and metastases.** Axillary lymph node metastases and intramammary tumor spread introduce dielectric inhomogeneities with responses similar to the primary tumor, which can overlap and interfere with microwave detection in the 2–3 GHz range. These overlapping signals may mask the primary lesion, distort localization, or cause false positives, an effect further intensified by the limited spatial resolution at these frequencies [12, 46, 47].
- **Morphological variations.** Tumor morphological variations alter dielectric properties and affect microwave detection. Calcifications may enhance detectability due to higher permittivity and conductivity, whereas dense fibrosis reduces dielectric contrast and weakens signals. Necrosis introduces heterogeneous scattering, while edema, cystic changes, and increased vascularization generally increase permittivity and conductivity. Overall, tissue heterogeneity can either improve or degrade microwave tumor detection [36, 46, 48, 49].
- **Torso and contralateral breast effects.** Included a qualitative analysis based on published microwave breast imaging studies, which demonstrate that tumor detection remains feasible even in the presence of torso and contralateral breast contributions through appropriate signal processing techniques such as background subtraction, normalization against reference scans, and multi-position antenna measurements [45, 49, 50, 51].
- **Future validation with realistic phantoms.** Planned work includes testing with anatomically realistic, heterogeneous, and multi-lesion phantoms incorporating primary tumors and metastatic nodes to improve discrimination of multiple dielectric anomalies.

6. Conclusion and future work

In conclusion, the purpose of this study is to evaluate the ability of a microwave breast detection system to identify dielectric inhomogeneities associated with malignant breast tumors and to assess its potential use as a non-ionizing mass-screening tool for differentiating normal from potentially pathological breast tissue.

This paper presented the design and simulation of a patch antenna for detecting and identifying tumors within breast tissue, using HFSS (High-Frequency Structure Simulator) to model the antenna integrated with a breast phantom. The study highlights the use of a moderate operating frequency of 2,4 GHz, which is considerably lower than frequencies used in other studies, sometimes reaching 23 GHz or higher [52], reducing potential health risks associated with electromagnetic exposure.

The theoretical results obtained with the proposed antenna configuration are promising, demonstrating its potential effectiveness for non-invasive breast tumor detection. As a future perspective, these findings require validation through practical implementation and experimental testing to assess real-world performance.

Further research could also explore optimization of antenna materials, use of multilayer breast phantoms, and integration with advanced imaging algorithms to enhance detection sensitivity and tumor localization accuracy.

We emphasize that microwave screening remains complementary to established staging modalities (ultrasound, MRI, PET/CT) for metastatic assessment.

REFERENCES

1. Umar. A, Atabo. S. A. review of imaging techniques in scientific research/ clinical diagnosis. // MOJ Anat Physiol, 2019, vol. 6, no 5, p. 175-83. DOI: 10.15406/mojap.2019.06.00269
2. Hussain, S., Mubeen, I., Ullah, N., Shah, S. S. U. D., Khan, B. A., Zahoor, M.,. & Sultan, M. A. (2022). Modern diagnostic imaging technique applications and risk factors in the medical field: a review.// BioMed research international, 2022(1), 5164970. PMID: 35707373 PMCID: PMC9192206 DOI: 10.1155/2022/5164970
3. Rana SP, Dey M, Tiberi G, Sani L, Vispa A, Raspa G, Duranti M, Ghavami M, Dudley S. Machine Learning Approaches for Automated Lesion Detection in Microwave Breast Imaging Clinical Data. Scientific Reports. 2019;9:10510. doi:10.1038/s41598-019-46974-3
4. Khan, A. Q., Touseeq, M., Rehman, S., Tahir, M., Ashfaq, M., Jaffar, E., & Abbasi, S. F. (2025). Advances in breast cancer diagnosis: A comprehensive review of imaging, biosensors, and emerging wearable technologies. Frontiers in Oncology, 15, 1587517. https://doi.org/10.3389/fonc.2025.1587517.
5. Sasada, S., Oda, N., Fukuda, H., Fujita, H., Okano, Y., Kondoh, T., et al. (2020). Microwave breast imaging using rotational bistatic impulse radar for the detection of breast cancer: Protocol for a prospective diagnostic study. JMIR Research Protocols, 9(10), e17524. https://doi.org/10.2196/17524
6. Shadrack O. A, John A. H, Graham. B, Yang. W. Portable noninvasive technologies for early breast cancer detection: A systematic review. Computers in Biology and Medicine, Volume 182, November 2024, 109219. https://doi.org/10.1016/j.compbiomed.2024.109219
7. Chishti, A. R., Aziz, A., Qureshi, M. A et al. Advances in antenna-based techniques for detection and monitoring of critical chronic diseases: A comprehensive review. //IEEE Access, (2023). 11, 104463-104484. DOI 10.1109/ACCESS.2023.3316149
8. Mahfuz, M. H., Mahfouz, A. M., Baladi, E., et al. Microstrip Patch Antennas for Breast Tumor/Cancer Cell Detection–Challenges, Designs and Future Opportunities: A Review.// IEEE Access. (2024). DOI 0.1109/ACCESS.2024.3496117
9. Saravanan, S., Haimavathi, K. U., & Aafizaa, K. Biomedical Antenna Design: Micro strip Patch Antennas for Wearable and Implantable Healthcare Applications—A Review.// Biomedical Materials & Devices, (2025). 1-11. DOI: 10.1007/s44174-025-00299-0

10. Govind. A, Paramjot. M, Ameya. S, et al. Systemic Overview of Microstrip Patch Antenna's for Different Biomedical Applications. // National library of Medicine, Adv Pharm Bull. 2020 Jul 1;11(3):439–449. doi: 10.34172/apb.2021.051
11. Guetaf, B. Design of a New Antenna for Biomedical Applications. // Doctoral dissertation. (2024). University of 8 Mai 1945 Guelma. Algeria
12. Wang, L. Microwave imaging and sensing techniques for breast cancer detection. // Micromachines, (2023). 14(7), 1462. https://doi.org/10.3390/mi14071462.
13. El Misilmani, H. M., Naous, T., Al Khatib, S. K., et al. A survey on antenna designs for breast cancer detection using microwave imaging.// IEEE Access, (2020). 8, 102570-102594. DOI: 10.1109/ACCESS.2020.2999053
14. Wilkinson, L., & Gathani, T. Understanding breast cancer as a global health concern. // The British journal of radiology, (2022). 95(1130), 20211033. DOI: 10.1259/bjr.20211033
15. Houghton, S. C., & Hankinson, S. E. Cancer progress and priorities: breast cancer. Cancer epidemiology.// biomarkers & prevention, (2021). 30(5), 822-844. DOI: 10.1158/1055-9965.EPI-20-1193
16. Haider, R. Anatomy of the Breast. //International Journal of Scientific Multidisciplinary Research, (2023). 1(5), 401-22. https://doi.org/10.55927/ijsmr.v1i5.4394
17. Zoya, G, Alethea, R, David, W, Jacki, L, M, et al. Maternal Factors, Breast Anatomy, and Milk Production During Established Lactation—An Ultrasound Investigation.// J Imaging. (2025). Sep 12;11(9):313. doi: 10.3390/jimaging11090313
18. Biswas, S. K., Banerjee, S., Baker, G. W, et al. The mammary gland: basic structure and molecular signaling during development.// International Journal of Molecular Sciences, (2022). 23(7), 3883. PMID: 35409243 PMCID: PMC8998991 DOI: 10.3390/ijms23073883
19. Schenkel, J. M., & Pauken, K. E. Localization, tissue biology and T cell state implications for cancer immunotherapy. // Nature Reviews Immunology, (2023). 23(12), 807-823. PMID: 37253877 PMCID: PMC11448857 DOI: 10.1038/s41577-023-00884-8
20. Mohcene. A. (2022). Study and Design of a New Antenna.// Master, University May 8, 1945 Guelma,. Algeria
21. Periferakis, A., Periferakis, K., Iftime, A., et al. Detection of Acupuncture Points and Meridians Based on their Electrical Properties: Current Evidence and Future Research Perspectives. // Rom. J. Mil. Med, (2025). 128, 378-400. DOI: 10.55453/rjmm.2025.128.5.2
22/ Jia, B., Huang, H., Dong, Z., Ren, X., et al. Degradable biomedical elastomers: paving the future of tissue repair and regenerative medicine. //Chemical Society Reviews, (2024). 53(8), 4086-4153. https://doi.org/10.1039/D3CS00923H
23. Fan, W., Hou, S., & Zhou, Z. The Duck 1000 Genomes Project: Achievements and perspectives.// Animal Research and One Health, (2024). 2(4), 366-376. https://doi.org/10.1002/aro2.89
24. Muñoz Taboada, G., Dahis, D., Dosta, P., et al. Sprayable hydrogel sealant for gastrointestinal wound shielding.// Advanced Materials, (2024). 36(24), 2311798. https://doi.org/10.1002/adma.202311798
25. Thomson, R. E., & Emery, W. J. Data analysis methods in physical oceanography.// Edition 4. Elsevier. (2024).
26. Ahmad. A. A, Allan. M. A, Mohd. N. M. Y, et al. Existing and Emerging Breast Cancer Detection Technologies and Its Challenges: A Review.// Appl. Sci. 2021, 11(22), 10753; https://doi.org/10.3390/app112210753.
27. Kenneth R.F, Herman P.S, Dielectric properties of tissues and biological materials: acritical review, department of bioengineering university of Pennsylvania, volume 17 Issue 1 1989
28. Coey. J. M. D, Stuart S.P. P. Handbook of Magnetism and Magnetic Materials. // Springer First Online, 02 September 2021
29. Tsabeeh. S. M. M, Adnan. M, Salah. M. M, et al. Enhancing Multispectral Breast Imaging Quality through Frame Accumulation and Hybrid GA-CPSO Registration.// Bioengineering 2024, 11(12), 1281; https://doi.org/10.3390/bioengineering11121281
30. Tale. S, Sarmad. N. M. Sahar, S. et al. Ultra-Wideband (UWB) Antennas for Breast Cancer Detection with Microwave Imaging: A Review,// Results in Engineering, (2025) vol. 25, no. 4, 104167, Mar. 2025, DOI: 10.1016/j.rineng.2025.104167.
31. Şahin. Y, Muhammed. B. K. Breast Cancer Detection Using a High-Performance Ultra-Wideband Vivaldi Antenna in a Radar-Based Microwave Breast Cancer Imaging Technique,// Applied Sciences, (2025) vol. 15, no. 11, 6015, 2025, DOI: 10.3390/app15116015.
32. Islam. M. T., Mahmud. M. Z., Islam, M. T et al, A Low-Cost and Portable Microwave Imaging System for Breast Tumor Detection Using UWB Directional Antenna Array.// Scientific Reports, (2019) vol. 9, 51620, 2019, DOI: 10.1038/s41598-019-51620-z.
33. Mariya. L, Dijana. P, Leah. M et al. A Large-Scale Study of the Ultra-Wide Band Microwave Dielectric Properties of Normal, Benign and Malignant Breast Tissues Obtained from Cancer Surgeries.// Physics in Medicine and Biology, (2007) vol. 52, pp. 6093–6115, 2007, DOI: 10.1088/0031-9155/52/20/002.
34. Yasmine. E. H, Mohamed. B, Abdelouahab. E.H et al. Parametric Study and Design of Ultra-Wideband Planar Microstrip Antenna for Breast Tumor Detection. //International Journal of Advanced Research (IJAR), 2016, DOI: 10.21474/IJAR01/3066.
35. Origlia, C., Rodriguez-Duarte, D. O., Tobon Vasquez, J. A et al. Review of microwave near-field sensing and imaging devices in medical applications. Sensors, (2024). 24(14), 4515. https://doi.org/10.3390/s24144515
36. Cheng, Y., & Fu, M. (2018). Dielectric properties for non-invasive detection of normal, benign, and malignant breast tissues using microwave theories. *Thoracic Cancer, 9*(4), 459–465. https://doi.org/10.1111/1759-7714.12605
37. Bah, M. H., Hong, J. S., & Jamro, D. A. (2015). Study of breast tissues dielectric properties in UWB range for microwave breast cancer imaging. In International Conference on Computer Information Systems and Industrial Applications (CISIA 2015) (pp. 473–475). DOI 10.2991/cisia-15.2015.129
38. Deepshikha. B, Phadungsak. R and Krit J. Microwave Imaging for Breast Cancer Detection- A Comprehensive Review.// Engineered Science Publisher LLC 2024 DOI: https://dx.doi.org/10.30919/es1116
39. Jinying. W, Shuical. W, Zeyi. W. Influences of blood flow parameters on temperature distribution during liver tumor microwave ablation.// Front. Biosci. (Landmark Ed) 2021, 26(9), 504–516; https://doi.org/10.52586/4963
40. Koutar. H. A, Ayoub. M. Creation, Simulation, Realization and Analysis of a Planar Antenna (Microstrip Patch Antenna).// License, Oum el baoughi, Larbi Ben M'Hidi University, 2022.
41. Zahra. K. Développement d'antennes pour la détection de tumeurs cancéreuses.// Liban, Doctoral dissertatio Universite libanaise, 2018
42. Fawzia. A. A, Askin. D. A novel textile-based UWB patch antenna for breast cancer imaging.// Physical and Engineering Sciences in Medicine (2024) 47:851–861. https://doi.org/10.1007/s13246-024-01409-w
43. Elsheikh, D. and Eldamak, A.R. Microwave Textile Sensors for Breast Cancer Detection.// 38th National Radio Science Conference (NRSC), Mansoura, 27-29 July 2021, 288-294. https://doi.org/10.1109/NRSC52299.2021.9509829
44. Xiaoyou. L, Yifan. C, Zheng, G et al. Ultra-Wideband Textile Antenna for Wearable Microwave Medical Imaging Applications.//. February 2020 IEEE Transactions on Antennas and Propagation PP(99):1-1. DOI: 10.1109/TAP.2020.2970072
45. Fernández-Aranzamendi, E. G., Castillo-Araníbar, P. R., San Román Castillo, E. G., Oller, B. S., Ventura-Zaa, L., Eguiluz-Rodriguez, G., González-Posadas, V., & Segovia-Vargas, D. (2024). Dielectric characterization of ex-vivo breast tissues: Differentiation of tumor types through permittivity measurements. *Cancers, 16*(4), 793. https://doi.org/10.3390/cancers16040793.
46. Lazebnik et al. measured significant dielectric property differences across breast tissue types in the microwave band, forming a foundational basis for imaging contrast (e.g., malignant vs. normal tissue) DOI: 10.3389/fphys.2017.00533 (review citing Lazebnik et al.) MDPI
47. Lazebnik, M., Zhu, C., Palmer, G. M., Harter, J., Sewall, S., Ramanujam, N., & Hagness, S. C. (2008). Electromagnetic spectroscopy of normal breast tissue specimens obtained from reduction surgeries: Comparison of optical and microwave properties. IEEE Transactions on Biomedical Engineering, 55(10), 2444–2451. https://doi.org/10.1109/TBME.2008.925700
48. Garrett, J. D., & Fear, E. C. (2015). Average dielectric property analysis of complex breast tissue with microwave transmission measurements. Sensors, 15(1), 1199–1216. https://doi.org/10.3390/s150101199
49. Aleksandar. J, Ibrahim. A, Mehmet. C, Onur. B, Mustafa .E .A. Microwave Breast Lesion Classification – Results from Clinical Investigation of the SAFE Microwave Breast Cancer System. Academic Radiology, Volume 30, Supplement 2, September 2023, Pages S1-S8. https://doi.org/10.1016/j.acra.2022.12.001
50. Shea, J. D., Kosmas, P., Hagness, S. C., & Van Veen, B. D. (2010). Three-dimensional microwave imaging of realistic numerical breast phantoms via a multiple-frequency inverse scattering technique. *Medical Physics, 37*(8), 4210–4226. https://doi.org/10.1118/1.3443569.
51. Särestöniemi, M., Singh, D., Dessai, R., Heredia, C., Myllymäki, S., & Myllylä, T. (2024). Realistic 3D phantoms for validation of microwave sensing in health monitoring applications. **Sensors**, 24(6), 1975. https://doi.org/10.3390/s24061975.
52. Allin. J. D, Gopika. S, Sobiya, S. M et al . Breast Cancer Detection Using Patch Antenna.// 2nd International Conference on Advancements in Electrical, Electronics, Communication, Computing and Automation (ICAECA) 2023, DOI: 10.1109/ICAECA56562.2023.10200909.

Конфликт интересов. Авторы заявляют об отсутствии конфликта интересов.
Финансирование. Исследование не имело спонсорской поддержки.
Участие авторов. Статья подготовлена с равным участием авторов.
Поступила: 20.06.2026. Принята к публикации: 25.07.2026.

Conflict of interest. The authors declare no conflict of interest.
Financing. The study had no sponsorship.
Contribution. Article was prepared with equal participation of the authors.
Article received: 20.06.2026. Accepted for publication: 25.07.2026.